



LAWRENCE  
LIVERMORE  
NATIONAL  
LABORATORY

# Modeling Techniques Used to Analyze Safety of Payloads for Generic Missile Type Weapons Systems During an Indirect Lightning Strike

M. P. Perkins, M. M. Ong, E. W. Crull, C. G. Brown Jr.

July 22, 2009

31st Annual Antenna Measurement Techniques Association  
Symposium  
Salt Lake City, UT, United States  
November 1, 2009 through November 6, 2009

## **Disclaimer**

---

This document was prepared as an account of work sponsored by an agency of the United States government. Neither the United States government nor Lawrence Livermore National Security, LLC, nor any of their employees makes any warranty, expressed or implied, or assumes any legal liability or responsibility for the accuracy, completeness, or usefulness of any information, apparatus, product, or process disclosed, or represents that its use would not infringe privately owned rights. Reference herein to any specific commercial product, process, or service by trade name, trademark, manufacturer, or otherwise does not necessarily constitute or imply its endorsement, recommendation, or favoring by the United States government or Lawrence Livermore National Security, LLC. The views and opinions of authors expressed herein do not necessarily state or reflect those of the United States government or Lawrence Livermore National Security, LLC, and shall not be used for advertising or product endorsement purposes.

# Modeling Techniques Used to Analyze Safety of Payloads for Generic Missile Type Weapons Systems During an Indirect Lightning Strike

Michael P. Perkins<sup>1</sup>, Mike M. Ong<sup>1</sup>, Eric W. Crull<sup>2</sup>, and Charles G. Brown Jr.<sup>1</sup>

<sup>1</sup>Lawrence Livermore National Laboratory, Livermore, CA, USA

<sup>2</sup>Formerly of Lawrence Livermore National Laboratory

Emails: [perkins22@llnl.gov](mailto:perkins22@llnl.gov), [ong1@llnl.gov](mailto:ong1@llnl.gov), [brown207@llnl.gov](mailto:brown207@llnl.gov)

## ABSTRACT

During lightning strikes buildings and other structures can act as imperfect Faraday Cages, enabling electromagnetic fields to be developed inside the facilities. Some equipment stored inside these facilities may unfortunately act as antenna systems. It is important to have techniques developed to analyze how much voltage, current, or energy dissipation may be developed over valuable components. In this discussion we will demonstrate the modeling techniques used to accurately analyze a generic missile type weapons system as it goes through different stages of assembly.

As work is performed on weapons systems detonator cables can become exposed. These cables will form different monopole and loop type antenna systems that must be analyzed to determine the voltages developed over the detonator regions. Due to the low frequencies of lightning pulses, a lumped element circuit model can be developed to help analyze the different antenna configurations. We will show an example of how numerical modeling can be used to develop the lumped element circuit models used to calculate voltage, current, or energy dissipated over the detonator region of a generic missile type weapons system.

**Keywords:** Analysis, Damage, EMI/EMC, Lightning, Modeling

## 1. Introduction

Over the past several years a probabilistic methodology has been developed to determine the vulnerability of high explosive (HE) systems stored in DOE facilities to the indirect lightning threat [1]. These facilities have been turned into Faraday cages that prevent the current of a lightning strike from attaching directly to HE systems [2]. Unfortunately, these facilities may have conductive penetrations or discontinuities in the structure of the Faraday cage. This leads to EM-fields developed inside the structures. An example of EM-fields developed inside such a facility that has been struck by lightning is shown in Fig. 1. In this example there is a discontinuity in the conductive structure between the walls and roof.

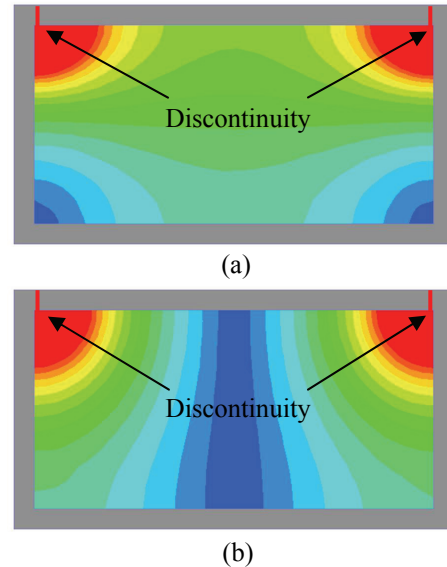


**Figure 1.** Magnitude of the (a) E-fields and (b) B-fields developed during a lightning strike in a facility that has a slot between the walls and roof (red represents high fields and blue low fields).

The lightning strike that is responsible for exciting the EM-fields in the facility can be modeled as a current source. It is known that lightning is statistical in both its parameters that define the current pulse, as well as where strikes occurs [3]. Because we would like to make sure that operations are safe under extreme lightning conditions, we have used values recommended in [3] for a 1% lightning strike. Some of these parameters are shown in Table 1. As one can see in the table, one lightning strike consists of several return strokes (pulses of current).

**Table 1.** Parameters used to characterize lightning for an average (50%) and extreme (1%) lightning strike [3].

	50%	1%
Peak Current (kA)	30	200
Maximum Rate of Rise (kA/ $\mu$ s)	150	400
Decay Time to Half Max ( $\mu$ s)	50	10-500
Number of Return Strokes	4	>20

It is common to represent the return stroke using either the double exponential or Heidler model [4, 5]. These are represented in Fig. 2a for parameters of 1% lightning. By taking the Fourier transform of these pulses, shown in Fig. 2b, one can see that the pulses are low frequency. This simplifies the analysis considerably for a couple of reasons. One is that a quasi-static analysis can be performed, assuming that the facility is not too large [6]. This makes it easier to determine the time varying fields in the facility [6]. The phenomena of interest vary temporally as the lightning pulse. Another reason why the low frequency of the pulse simplifies the analysis is that the monopole and loop type antenna systems that are formed are significantly smaller than the smallest wavelength of interest.

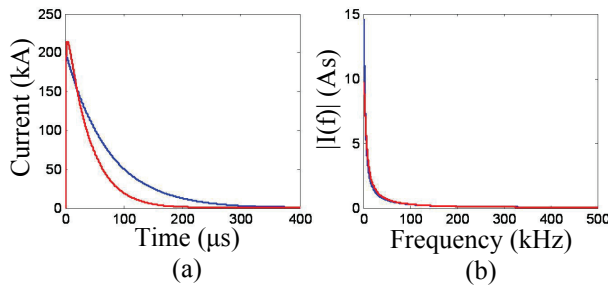


**Figure 2.** The (a) current pulse and (b) the Fourier transform of the pulse for the double exponential (blue) and the Heidler (red) representations of a return stroke.

After the EM-fields incident on the weapons system are found [6], configurations must be determined that might be susceptible to electromagnetic coupling. Figure 3 shows a simple missile type system that consists of a section for electronics and guidance, payload (HE), and propulsion. An electronic detonator is used to initiate the insensitive HE in the payload. The detonator cable is connected to an electrical firing unit (EFU), which sends a voltage pulse to initiate the detonator. When operating in its intended mode, the voltage of the pulse is between the two conductors of the detonator cable.

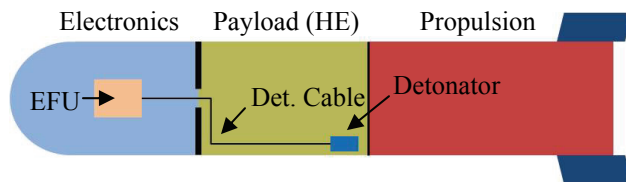


**Figure 3.** Generic missile type system composed of a section for electronics, payload (HE), and propulsion.

The fully assembled system shown in Fig. 3 is typically not sensitive to the indirect lightning threat because of shielding provided by the metal case of the missile. The threat occurs when this shielding is not present, such as when the payload is partially or fully assembled on a work stand. This configuration is illustrated in Fig. 4. In

this setup the detonator and part of detonator cable form a load and a section of transmission line (T-line). The other conductor of the T-line is the nearby metal case of the payload. The rest of the detonator cable, payload, and work stand form an antenna.

In Fig. 4b a close up of the detonator is shown. It is a simplified and scaled version of the electronic blasting cap discussed on p. 101 in [7]. The values for the relative permittivity used are typical values for several types of HE. The detonator cable is a coax that has a 1 mm radius outer conductor, surrounded by a 2 mm radius insulator with  $\epsilon_r = 2.0$  ( $\epsilon_r$  is the relative permittivity). The total length of the cable is 1 m.

In the unintended mode of operation the fields generated in the facility from the lightning strike are received by the antenna that is formed. The antenna can be either a monopole type antenna, as illustrated in Fig. 4a, or a loop type antenna, which can be formed when the free end of the detonator cable is connected to nearby metal. In the unintended mode of operation the conductors of the detonator cable and the bridge wire of the detonator are at the same potential. If the voltage between the metal case that surrounds the HE (at ground potential) and the detonator cable is too high, an electrical arc (spark) can form inside the detonator. If enough energy is dissipated in this arc, the sensitive HE in the detonator can initiate, which would lead to the insensitive HE in the payload going off. The voltage and energy strengths of different detonators are often found by testing.

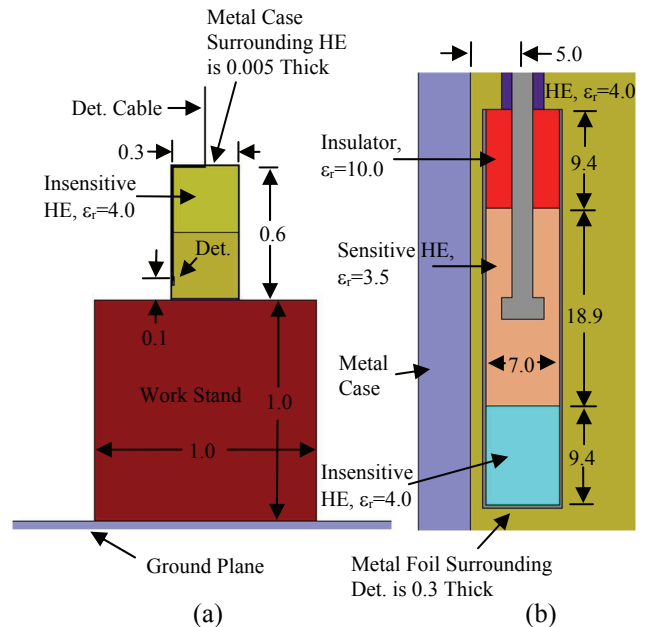


**Figure 4.** Dimensions and relative permittivity shown for a cross section of (a) the payload on a work stand in meters and of (b) the detonator region in millimeters.

In the remainder of this paper we will demonstrate how to find the open circuit voltage for the loop type antenna system, then the voltage over the detonator for monopole type antenna systems. We will make use of the full wave frequency solver HFSS and the electrostatic solver Maxwell [8] to model several important parameters. In the final section we will briefly discuss energy dissipation in possible arc's that are formed. For our analysis we will assume an extreme lighting strike to the facility. We will use the values given in [1] for the total EM-fields incident on the antenna systems. The maximum E-field is 10 kV/m, and the maximum derivative of the B-field is 2 kV/m<sup>2</sup>.

## 2. Loop Type Antenna Configurations

It is well known that the open circuit voltage of a loop antenna is found by integrating the derivative the B-field over the area of the loop, as shown in Eq. (1). It can also be found by integrating the E-field along a line between the two conductors that form the open circuit terminals of the antenna, as shown by Eq. (2).

$$V_{O.C.} = \int \frac{dB}{dt} \cdot dArea \quad (1)$$

$$V_{O.C.} = \int E_{Gap} \cdot dl \quad (2)$$

Because the quasi-static assumption is valid  $B = k \cdot i(t)$ , where  $k$  is some constant with time and  $i(t)$  is the current of the return pulse. The constant  $k$  can be found by relating the maximum current that excites the facility to the maximum B-field generated inside ( $k$  varies with position). After  $k$  is found, one can take the derivative of both sides, giving Eq. (3).

$$\frac{dB}{dt} = \alpha \frac{B_{max}}{i_{max}} \frac{di}{dt} \quad (3)$$

In Eq. (3)  $\alpha$  represents an enhancement factor, which takes into account perturbations of the field due to the presence of the work stand and payload. From Eq. (3) we see that the maximum dB/dt occurs at maximum di/dt, which was given in table 1. We assume for our example that the maximum of dB/dt without the work stand and payload present is 2 kV/m<sup>2</sup>, polarized normal to the loop. We will analyze the worst case configuration in which the top part of the payload is removed (both HE and outer metal case), leaving an exposed detonator cable of 0.8 m.

Figures 5a and 5b shows the results of placing a full loop in free space and a half loop above a ground plane for a length of cable 0.8 m long. The incident B-field is 1 mWb/m<sup>2</sup> and the frequency is 318.31 kHz. One can see that the presence of the cable does not alter the B-field

significantly. The open circuit voltage was found in HFSS using Eq. (2). The computed result for the full loop case was 101.9 V and for the half loop it was 203.8 V (twice as big due to twice the area). These values lead to negligible percent errors with theory.

Next, the configuration with the work stand and partly assembled payload was modeled. The results are shown in Fig. 5c. One can see that the antenna system has perturbed the local B-field. The open circuit voltage found using Eq. (2) was 381.3 V. The field is 1.33 times higher over the loop area (enhancement factor) than when the antenna system is not present. The area of the loop is 1.4 times the area of the half loop over the ground plane. If the enhancement factor and increased area of the loop in the configuration are neglected, it could potentially cause systems that are unsafe to pass a safety assessment. A future area of research is to include setups where the end of the detonator cable is capacitively coupled to the work stand rather than just conductively.

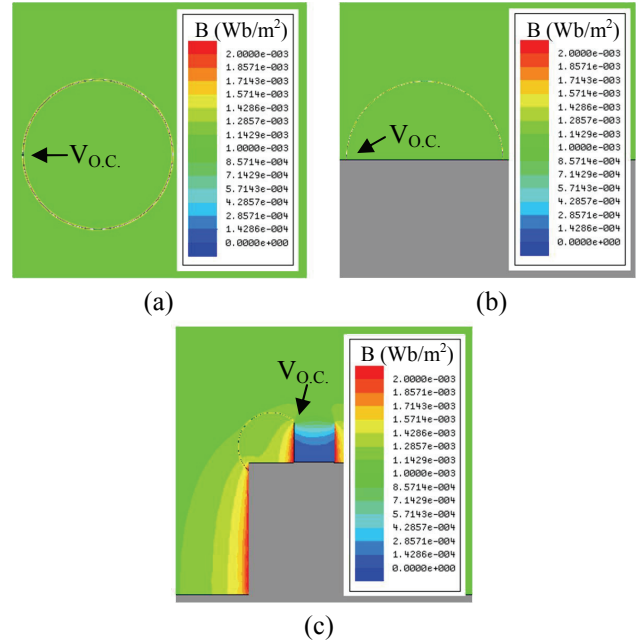


**Figure 5.** Magnitude of the B-field for (a) a full loop in free space, (b) a half loop above a ground plane, and (c) part of the payload and the work stand.

## 3. Monopole Type Antenna Configurations

Now that we have discussed loop type antennas, we will discuss monopole type antennas. E-fields are generated in the facilities due to inductive voltages. Because the

quasi-static assumption is valid  $E = k \cdot \frac{di}{dt}$ . The same reasoning used to derive Eq. (3) can be followed to obtain  $E(t)$ . As stated, we will assume that the maximum E-field

incident on the antenna is 10 kV/m, polarized parallel to the detonator cable.

Excitation of simple monopole antennas to low frequency pulses has been discussed elsewhere [9, 10]. It was shown in [10] that the simple lumped element circuit of Fig. 6 can be used to represent the monopole type antenna system for lightning pulses. In the circuit  $h_{\text{eff}}$  is the antenna effective height, and the C's represent capacitances of the different components in the system. The voltage over the detonator can be found with Eq. (4).

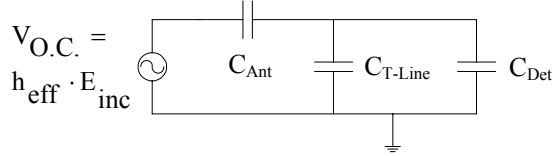


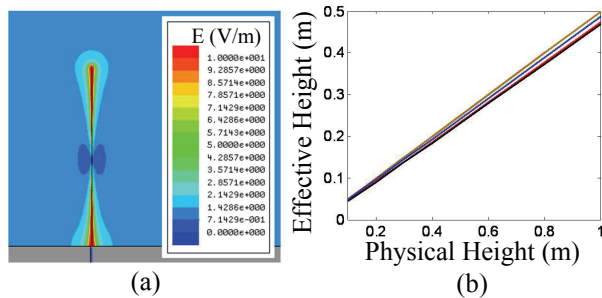
**Figure 6.** Electrical circuit used to represent monopole type antenna system for lightning pulses.

$$V_{\text{Det}} = \frac{h_{\text{eff}} \cdot E_{\text{incident}} C_{\text{Ant}}}{C_{\text{Ant}} + C_{\text{T-Line}} + C_{\text{Det}}} \quad (4)$$

To begin analyzing the system we use HFSS to compute  $h_{\text{eff}}$ . In HFSS we apply 1 V/m incident on the antenna at 500 kHz. The open circuit voltage of the antenna is computed using Eq. (2). Equation (5) can then be used to find  $h_{\text{eff}}$ .

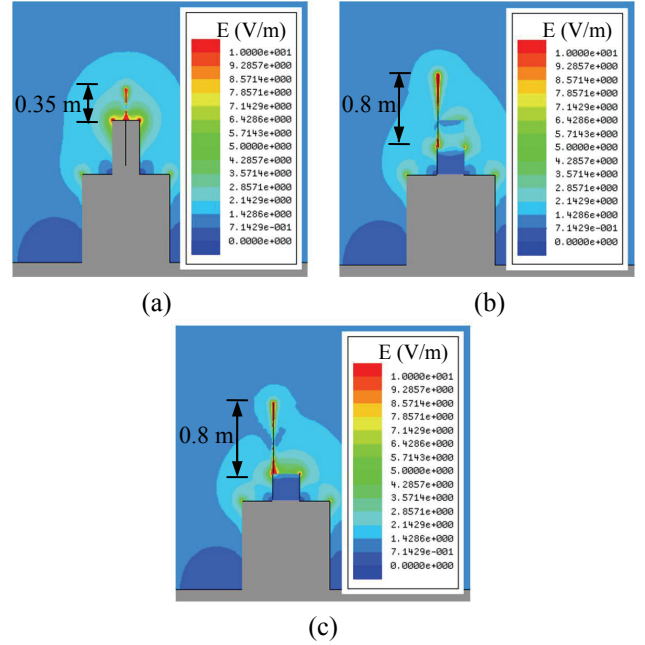
$$h_{\text{eff}} = \frac{V_{\text{O.C.}}}{E_{\text{incident}}} \quad (5)$$

Figure 7a shows the resultant E-field for a monopole above a ground plane used to compute  $h_{\text{eff}}$ . Figure 7b shows  $h_{\text{eff}}$  of a monopole above a ground plane, found several different ways, as well as  $h_{\text{eff}}$  of the detonator cable. The brown line represents physical height divided by 2, the blue line is the theoretical expression given by Eq. (B.3) in [10], the red line is the computed  $h_{\text{eff}}$  of the monopole using HFSS, and the black line is the computed  $h_{\text{eff}}$  for the detonator cable above a ground plane.



**Figure 7.** (a) E-field used to compute  $h_{\text{eff}}$  using HFSS and (b)  $h_{\text{eff}}$  of a monopole above a ground plane as well as  $h_{\text{eff}}$  for the detonator cable above a ground plane.

From Fig. 7b we can see that using this method to find effective height can be very accurate. Next, we use this method to find  $h_{\text{eff}}$  for a couple of configurations that the system may undergo during assembly. Figure 8 shows cross sectional views of the E-field used to compute  $h_{\text{eff}}$  as well as the length of exposed detonator cable. For the outer metal case fully on the payload (Fig. 8a)  $h_{\text{eff}} = 0.75$  m, for the upper part of the metal case removed (Fig. 8b)  $h_{\text{eff}} = 0.81$  m, and for the upper part of the metal case removed as well as the upper half of HE (Fig. 8c)  $h_{\text{eff}} = 1.12$  m. By comparing these effective heights to those shown in Fig. 7b for the cable, it is evident that the work stand and payload had a large effect on the results.



**Figure 8.** E-fields used to compute  $h_{\text{eff}}$  for (a) metal case on, (b) top of metal case removed, and (c) top of metal case and top part of HE removed.

Now that the driving voltage of the circuit has been determined, we will find the capacitances shown in Fig. 6. To compute capacitance we rely on the relationship between electrical energy in lumped form and in field form given in Eq. (6).

$$W_e = \frac{1}{2} CV^2 = \frac{1}{2} \int \epsilon_0 \epsilon_r E \cdot E d\text{Volume} \quad (6)$$

We will place the outer metal case of the payload and the work stand at 0 V and the conductor of the cable at 1 V. Then Maxwell is used to compute the integral in Eq. (6). This result is multiplied by 2 to give the capacitance.

Figure 9a shows an example of the energy density used to compute the capacitance of a monopole antenna above a ground plane. Figure 9b shows the computed detonator



cable capacitance above a ground plane, computed capacitance of monopole, as well as the theoretical capacitance of a monopole given by Eq. (B.2) in [10]. As one can see the theoretical and computed capacitance of the monopole are in good agreement. Figure 10 shows the energy density used to calculate the capacitances of the antennas corresponding to the setups shown in Fig. 8. The computed capacitances for the configurations shown in Figs. 10a, 10b, and 10c are 4.51 pF, 12.78 pF, and 8.37 pF. By comparing these results with those shown in Fig. 9b, one can see that only the configuration shown in Fig. 10b was significantly different than the cable above a ground plane. This is due to the permittivity of the HE.

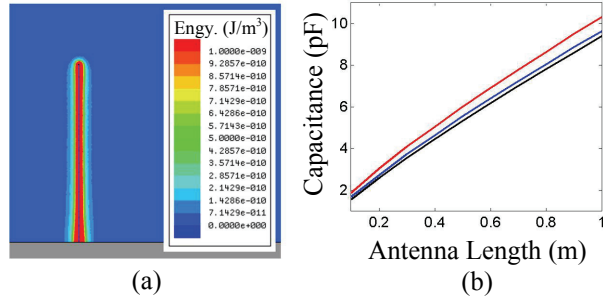


**Figure 9.** (a) Energy density used to compute capacitance of monopole and (b) theoretical (black) and computed (blue) capacitance of monopole as well as computed cable capacitance (red) above a ground plane.

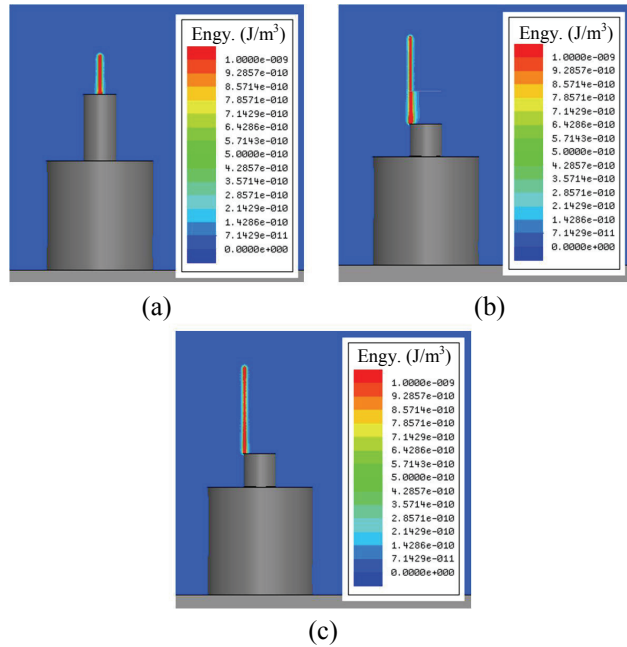


**Figure 10.** Energy density used to compute  $C_{Ant}$  for (a) metal case on, (b) top of metal case removed, and (c) top of metal case and top part of HE removed.

The next capacitance to compute in the circuit is for the T-line. The T-line is formed between the metal case surrounding the HE of the payload and the cable. The T-line can be modeled as a cable over a ground plane. For this example the curvature of the metal case has little effect on the capacitance. Figures 11a and 11b show the energy density used to compute capacitance for a conductor above a ground plane and for the detonator cable surrounded by HE above a ground plane. Figure 11c shows the theoretical capacitance for Fig. 11a (black), the computed capacitance for Fig. 11a (blue), computed capacitance of Fig. 11b if  $\epsilon_r=1$  (brown), and computed capacitance of Fig. 11b for  $\epsilon_r=4$  (red). For the two configurations with the metal case off the capacitance is given by  $0.2 \text{ m} * 74.0 \text{ pF/m} = 14.8 \text{ pF}$ . For the configuration with the metal case on the capacitance is given by  $0.64 \text{ m} * 74.0 \text{ pF/m} = 47.36 \text{ pF}$ . When the case is on there is also 0.01m of T-line composed of the cable going through a hole in the metal case and a small portion vertical to the ground plane (illustrated in Fig. 3). This section of the T-line has a capacitance of 0.89 pF.

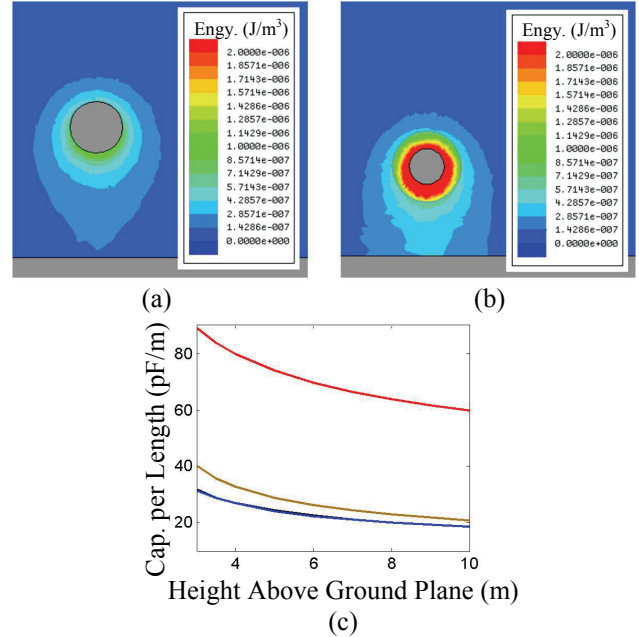


**Figure 11.** (a) Energy density used to compute capacitance of conductor above ground plane, (b) energy density used to compute capacitance of detonator cable surrounded by HE above a ground plane, and (c) variation of capacitance with height above a ground plane for several different situations of interest (red is T-line).

The final capacitance to compute in the circuit is for the detonator. The energy density used to find this is shown in Fig. 12. The metal foil of the detonator is floating. The detonator is excited by a length of T-line of known capacitance, which can be subtracted out to give a capacitance of 4.13 pF for the detonator.

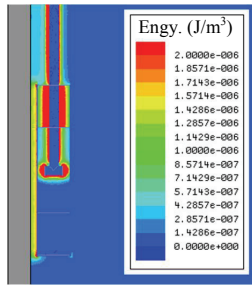


**Figure 12.** Energy density used to find capacitance of the detonator.

Now that we have the values for all of the components of the circuit shown in Fig. 6, we can compute the voltage at the detonator using Eq. (4). For the three different configurations represented by Figs. 10a, 10b, and 10c the voltages over the detonator are calculated to be 597 V, 3460 V, and 3300 V. To test the analysis procedure, the three different configurations were fully modeled using HFSS (antenna, T-line, and detonator all included in simulation). The percent difference between the values calculated above and the full simulation were less than 5% for all configurations!

#### 4. Arc Energy Calculations

If the voltage developed over the detonator for the loop or monopole type antenna system is too high, an arc may form. Determining the resistance of an arc is a complicated nonlinear time dependent problem and is an active area of research [11, 12]. To complete a safety analysis one may be able to bound the maximum energy dissipated in a potential arc by using optimization and performing parametric studies.

For simplicity, we will assume that the arc is a constant resistance of  $1\ \Omega$ . We will also assume that there is only one return stroke that is represented by the simple Heidler waveform shown in Fig. 2a. For the configuration with half the HE removed, the energy dissipated in the  $1\ \Omega$  resistor will be computed. For the monopole type system we find that the energy dissipated is approximately  $10\ \mu\text{J}$ , and for the loop type system it is approximately  $10\ \text{mJ}$  (used loop inductance of  $1\ \mu\text{H}$ ). This demonstrates that even though the monopole type antenna system develops a higher voltage over the detonator than the loop type antenna system, the energy dissipated in a possible arc is much less.

#### 5. REFERENCES

- [1] M.M. Ong, M.P. Perkins, C.G. Brown Jr., E.W. Crull, and R.D. Streit, "Indirect Lightning Safety Assessment Methodology," LLNL-TR-414094, June 2009.
- [2] T.J. Clancy, C.G. Brown Jr., M.M. Ong, and G.A. Clark, "Lightning Protection Certification for High

Explosive Facilities at Lawrence Livermore National Laboratory," 2006 IEEE Ant. Prop. Soc. Conf., Albuquerque NM.

- [3] R.J. Fisher, and M.A. Uman, "Recommended Baseline Direct-Strike Lightning Environment for Stockpile-to-Target Sequences," SAND89-0192, May 1989.

- [4] A. Andreotti, U. De Martinis, L. Verolio, "Comparison of Electromagnetic Field for two Different Lightning Pulse Current Models," Euro. Trans. Elec. Power, Vol. 11, No. 4, pp. 221, July/Aug. 2001.

- [5] M.A. Uman, V.A. Rakov, J.O. Elisme, D.M. Jordan, C.J. Biagi, and J.D. Hill, "Update Direct-Strike Lightning Environment for Stockpile-to-Target Sequence," LLNL-SR-407603, Sept. 2008.

- [6] Private communications with Kimball O. Merewether of Sandia National Laboratories.

- [7] J. Ledgard, *The Preparatory Manual of Explosives, Third Edition*, 2007.

- [8] HFSS and Maxwell are available from Ansoft LLC, <http://www.ansoft.com/>.

- [9] H.J. Schmitt, C.W. Harrison Jr., and C.S. Williams Jr., "Calculated and Experimental Response of Thin Cylindrical Antennas to Pulse Excitation," IEEE Trans. On Ant. Prop., Vol. 14, No. 2, pp. 120, March 1966.

- [10] E.W. Crull, C.G. Brown Jr., M.P. Perkins, and M.M. Ong, "Experimental Validation of Lightning-Induced Electromagnetic (Indirect) Coupling to Short Monopole Antennas," LLNL-TR-405954, August 2008.

- [11] R. Montano, M. Becerra, V. Cooray, M. Rahman, and P. Liyanage, "Resistance of Spark Channels," IEEE Trans. Plasma Sci., Vol. 34, No. 5, pp. 1610, Oct. 2006.

- [12] Private communications with Laura K. Tully of Lawrence Livermore National Laboratory.

#### 6. ACKNOWLEDGMENTS

The authors wish to thank Ronald D. Streit and Constantine A. Hrousis for providing funding for this study. Colleagues James F. McCarrick, David Steich, Laura K. Tully, and Alvin E. Travao of Lawrence Livermore National Laboratory for several interesting conversations related to this work. Finally, we would also like to thank Kimball O. Merewether of Sandia National Laboratories for his input related to this work.

This work performed under the auspices of the U.S. Department of Energy by Lawrence Livermore National Laboratory under Contract DE-AC52-07NA27344.